Available online at www.sciencedirect.com
SCIENCE DIRECT
Journal of Catalysis 235 (2005) 114–127
JOURNAL OF CATALYSIS
www.elsevier.com/locate/jcat

Lean hydrocarbon selective catalytic reduction over dual pore system zeolite mixtures

Martin Petersson [a,b,c], Thomas Holma [a,d], Bengt Andersson [a,b], Edward Jobson [a,b,c], Anders Palmqvist [a,c,d,*]

[a] *Competence Centre for Catalysis, Chalmers University of Technology, SE-412 96 Göteborg, Sweden*
[b] *Department of Chemical Engineering and Environmental Science, Chalmers University of Technology, SE-412 96 Göteborg, Sweden*
[c] *Volvo Technology AB, Chalmers Science Park, SE-412 88 Göteborg, Sweden*
[d] *Department of Materials and Surface Chemistry, Chalmers University of Technology, SE-412 96 Göteborg, Sweden*

Received 10 May 2005; revised 15 July 2005; accepted 18 July 2005

Available online 22 August 2005

Abstract

Physical mixtures of CuFER and HZSM-5, CuFER and AgMOR, and CoFER and AgMOR zeolites were investigated as potential dual pore system catalysts for continuous lean NO_x reduction with propene or isooctane as reducing agents. The effects of variations in temperature and oxygen concentrations were studied using steady-state experiments. Despite lower rates of external and internal mass transfer, the mixture of CuFER and HZSM-5 was found to have the highest NO_x reduction activity with isooctane as the reducing agent. A maximum NO_x reduction of about 40% was found for this catalyst at 350 °C and 12% oxygen. In this case, the CuFER extrudate acted as an NO oxidation catalyst, and the NO_2 formed was reduced by the isooctane in the HZSM-5 extrudate. The better performance of the CuFER and HZSM-5 mixture compared with the other mixtures was attributed to a higher selectivity for NO_2 to form nitrogen in the reduction reaction. When propene was used, the two mixtures containing CuFER showed similar reduction activity with a maximum conversion of about 65% at 370 °C and 2% oxygen. In contrast with the isooctane, the NO_x reduction with propene occurred primarily in the extrudate containing ferrierite. Again, the selectivity of NO_2 to form nitrogen governed the overall NO_x reduction.

Keywords: HC-SCR; Zeolites; Propene; Isooctane; NO_x reduction; Dual pore system catalyst

1. Introduction

Global warming is probably the greatest environmental threat today. This fact is internationally recognized by the United Nations Framework Convention of Climate Change [1], a document currently ratified by 193 nations [2]. To meet this threat, the nations that have ratified the Kyoto Protocol [3] have pledged to reduce their collective emissions of greenhouse gases by at least 5% below the 1990 level in the time period 2008–2012. To contribute to this target, the European vehicle industry has made the commitment to reduce the average carbon dioxide emissions for new cars to 140 g/km in 2008, a 25% reduction from the 1995 level [4].

Diesel and lean burn technologies have a high potential to lower fuel consumption and thus lower carbon dioxide emissions. The drawbacks to these technologies are the higher emissions of particulate matter and the problems in reducing the emissions of NO_x. To control particulate emissions, particulate traps such as the CRT system [5] have been implemented in vehicles. For NO_x emission control, several techniques are currently under development [6]. A potentially useful technology is hydrocarbon-selective catalytic reduction (HC-SCR). This technique can use the fuel as a reducing agent, precluding the need for an additional reducing agent on-board, as in urea SCR. In addition, high-

* Corresponding author. Fax: +46-31-160062.
E-mail address: adde@chem.chalmers.se (A. Palmqvist).

0021-9517/$ – see front matter
doi:10.1016/j.jcat.2005.07.018

$$NO + (1/2)O_2 \rightleftarrows NO_2 \quad (1)$$

$$NO_2 + HC \not\rightarrow N_2 + \text{oxidized HC} + CO_2 + CO + H_2O \quad (2a)$$

$$NO_2 + HC \not\rightarrow NO + \text{oxidized HC} + CO_2 + CO + H_2O \quad (2b)$$

$$O_2 + HC \not\rightarrow \text{oxidized HC} + CO_2 + CO + H_2O \quad (3)$$

Fig. 1. Simplified reaction scheme for NO_x reduction over a dual pore system catalyst. Crossed over arrows indicate a non-balanced reaction.

temperature sulfur regeneration is not required, as for NO_x storage catalysts.

Several catalyst systems are active for HC-SCR [6]. Copper-exchanged zeolite ZSM-5 attracted attention in the early 1990s. However, this material has insufficient long-term stability and activity as well as a narrow operating temperature window, and water diminish its performance [7–9]. High oxygen concentrations also lower catalyst performance. It has been reported that a gas mixture consisting of 1000 ppm NO, 1000 ppm propene, and an oxygen concentration of 2% yields the highest NO_x reduction over CuZSM-5 [10]. In addition to CuZSM-5, other zeolite-based SCR systems have been evaluated. Metal-containing zeolites, such as CoZSM-5 [11,12] and FeZSM-5 [13,14], and acidic zeolites [15–19] have shown NO_x reduction activity with hydrocarbons. CoZSM-5 was found to be SCR active with methane, and FeZSM-5 showed good results with isobutane, even in the presence of sulfur and water. There have also been reports that mixtures of zeolites and metal oxides [20] can be used for the reduction of NO_x; for example, a mixture of Mn_2O_3 and SnZSM-5 was reported to give better NO_x reduction in the presence of water than in the absence of water.

Mixtures of zeolites with differing pore structures, termed dual pore systems, are also reported to be more active for NO_x reduction than the single components alone [21–23]. Combining platinum ferrierite with silver mordenite enhanced the NO_x reduction with isooctane as the reducing agent [21], and a mixture of cobalt ferrierite and acidic ZSM-5 was active for NO_x reduction with isobutane [23]. The mechanism suggested in the former article is that NO was selectively oxidized to NO_2 in the small-pore zeolite and, subsequently, reduced to nitrogen by the hydrocarbon in the large-pore zeolite [21].

Several reaction mechanisms for NO reduction with hydrocarbons over zeolite systems have been suggested, but most evidence currently supports that NO_2 acts as an intermediate in the reduction [9,19,24,25]. Based on these previous studies, the overall reduction reaction in dual pore system catalysts can be visualized by the simplified reaction scheme shown in Fig. 1. In reaction (1), NO is oxidized to NO_2. Depending on the oxygen concentration, this reaction is thermodynamically limited at high temperatures. The NO_2 is then reduced to either nitrogen (reaction (2a)) or back to NO with a hydrocarbon species (reaction (2b)). Some form of oxidized hydrocarbon species is also formed in these reactions. The oxidation of the hydrocarbon with oxygen (reaction (3)) competes with the reduction reaction. Although both NO oxidation and NO_2 reduction to nitrogen (reactions (1) and (2a)) may occur in a single zeolite component (for example [23]), the selectivity toward these reactions is not typically optimal in a single zeolite component, which is why the addition of a proper second component is beneficial. To minimize competition for the reducing agent between reactions (2a) and (3), it is desirable to suppress oxidation of the hydrocarbon with oxygen. This can be done by placing the oxidation catalyst for reaction (1) in a component with a low affinity for the hydrocarbon. In addition, the other component needs to have a high selectivity for reaction (2a) in comparison with reactions (2b) and (3), to achieve a high overall nitrogen formation.

In the present study, three new zeolite mixtures were evaluated as dual pore system catalysts. The mixtures consisted of a combination of three zeolite structures: ferrierite, mordenite, and ZSM-5. Of these three structures, ferrierite has the narrowest pores, followed by ZSM-5 and mordenite. The ferrierite structure was ion-exchanged with either copper or cobalt, mordenite was silver-exchanged, and ZSM-5 was in acidic form. Copper and cobalt was selected because they were expected to have suitable activity for NO oxidation.

The effect of temperature and oxygen concentration was investigated under stationary conditions with either propene or isooctane as the reducing agent. Propene was expected to readily access even the small-pore zeolite, with the bulkier isooctane able to enter only the large-pore zeolite. The dual pore system effect was thus expected to be detected only for isooctane. The results are discussed in the light of the suggested simplified reaction scheme shown in Fig. 1. Whenever zeolite samples are compared, the effect of diffusion limitation is of vital importance. In the current study, the zeolite crystal size and the average extrudate pore radius varied with crystal structure. The impacts of these co-variations were taken into account in the evaluation of the results.

2. Experiments

2.1. Sample preparation and characterization

Three zeolite types were used in this study: ferrierite, mordenite, and ZSM-5. All three of these zeolites were provided from their manufacturer in acidic form as 1.5-mm-diameter extrudates. The ferrierite extrudates were provided by Tosoh, and the mordenite and ZSM-5 were from Eka Chemicals. The ZSM-5 sample was used as received and is denoted as HZSM-5 throughout this paper. From the ferrierite extrudates, one batch of copper-exchanged samples and another batch of cobalt-exchanged samples were prepared; these samples are denoted as CuFER and CoFER. The mordenite extrudates were silver-exchanged and are denoted as AgMOR.

Table 1
Zeolite extrudate properties

Property	CuFER	CoFER	HZSM-5	AgMOR
Manufacturer	Tosoh	Tosoh	Eka	Eka
SiO_2/Al_2O_3 ratio	16.5	16.5	33	30
Ion/Al ratio (Ion = Cu, Co or Ag)	0.3433	0.0272	–	0.193
Extrudate diameter (mm)	1.5	1.5	1.5	1.5
Average extrudate length (mm)	6	6	6	6
Extrudate density (kg/m^3)	1110	1110	1048	1106
Binder type	Silica	Silica	Alumina	Alumina
Binder (wt%)	30	30	30	30
Crystal density (kg/m^3)	2110	2110	1894	2083
Average crystal size (μm)	1	1	10	0.5
BET surface area (m^2/g)	322.0	322.0	366.7	463.0
Total pore volume (ml/g)	0.3217	0.3217	0.2815	0.3368
Micropore area (m^2/g)	276.6	276.6	266.5	350.1
Micropore volume (ml/g)	0.1083	0.1083	0.1149	0.1388
Average pore radius excluding micropores (Å)	94.0	94.0	33.3	35.1
Extrudate porosity excluding micropores (–)	0.2369	0.2369	0.1747	0.2190

The metal ion exchange was conducted by first passing a 1 mol/dm^3 $NaNO_3$ solution through a 10 g extrudate bed in an ion-exchange column until the pH of the solution passing the bed was equal to the pH in the sodium solution. Thereafter, the sodium-exchanged samples were ion-exchanged with the desired ion. All of the metal salt solutions were 0.025 mol/dm^3 and consisted of $Cu(CH_3COO)_2$, $Co(NO_3)_2$, or $AgNO_3$. In each ion exchange, 3 dm^3 of the solution was used. After the exchange, the ion-exchange ratio was determined spectroscopically. The resulting metal ion/aluminum ratio is given in Table 1. In addition, SEM analysis (using a JEOL JSM-5200) was done to determine the zeolite crystal sizes, and nitrogen adsorption at −196 °C (using an ASAP 2010) was done to investigate the extrudate pore system sizes and BET area. The results of these evaluations are given in Table 1. For the ferrierite samples, the crystal size specification from the supplier is listed.

From these four zeolite extrudate batches, three zeolite mixtures were prepared: CuFER + AgMOR, CuFER + HZSM-5, and CoFER + AgMOR. Each mixture was prepared by mixing the two zeolite extrudate batches at a 50:50 wt% ratio (see Table 2).

2.2. Reactor experiments

The NO_x reduction experiments were performed in a vertically mounted metal tube reactor. The zeolite bed was placed between two sintered quartz frits, to distribute the gas evenly over the reactor cross-section. The gas entering the reactor was heated by a capillary pre-heater, and the reactor wall was heated by a metallic heating coil. The temperature was measured by thermocouples before and after the zeolite bed; separate temperature control units were used to regulate the temperature in the capillary preheater and the tube reactor. The average inlet temperatures were maintained within 3 °C of the setpoint.

Table 2
Zeolite mixture properties

Property	CuFER + AgMOR	CuFER + HZSM-5	CoFER + AgMOR
Weight (g)	8.9657	8.0906	8.5191
Weight ratio between components	1:1	1:1	1:1
Density (kg/m^3)	713	644	678

Four separate mass flow controllers (Brooks Instrument models 5850S and 5850E) were used to mix the reactor feed stream of nitrogen (99.996%), oxygen (99.95%), nitric oxide (99%), and propene (99.5%). A liquid mass flow controller (Bronkhorst Hi-Tec μ-Flow) was used to inject isooctane (99.5%) into the 120 °C hot gas feed just before the capillary preheater. To avoid condensation of isooctane, all tubes between the reactor and the analysis instruments were kept at 120 °C. The reactant and product gases were analyzed online using a chemiluminiscence detector (Eco Physics CLD 700 RE ht) for NO and NO_2, a gas phase Fourier transform infrared spectroscope (Gasmet FT-IR) for CO and CO_2, and a flame ionization detector (FID) (Signal Hydrocarbon Analyser Model 3000) for total hydrocarbon concentration.

The zeolite sample mixtures were heated to 500 °C in 6% oxygen and kept constant at that temperature for 30 min to condition the sample before the experiments were started. Continuous NO_x reduction with hydrocarbon was studied at steady-state temperatures of 500, 370, 350, 330, and 200 °C. The feed gas consisted of oxygen (varied between 0 and 12%), nitric oxide (1000 ppm), nitrogen (balance), and either propene (1067 ppm) or isooctane (400 ppm). The oxygen concentration was varied in the order 6, 10, 4, 2, 12, 0, and 8%. At both 0 and 6%, the system needed 20 min to stabilize, whereas 10 min was sufficient for the other concentrations. A total flow rate of 3240 ml/min was used, corresponding to a space velocity of 15 500 h^{-1}.

Temperature-programmed reaction ramps were performed immediately after the steady-state reaction measurements. The samples were cooled from 500 to 120 °C and saturated at 120 °C in a gas mixture consisting of nitric oxide (1000 ppm), propene (1067 ppm), oxygen (6%), and nitrogen (balance). The samples were degassed at 120 °C for 10 min and heated to 500 °C at 10 °C/min in a gas consisting of 6% oxygen with nitrogen as balance. The total flow rate was 3240 ml/min throughout these experiments.

3. Results and discussion

3.1. Impact of test conditions, external and intrapellet mass transfer

The NO_x reduction was evaluated for the three zeolite mixtures, using propene or isooctane as the reducing agent at different oxygen concentrations and temperatures. The

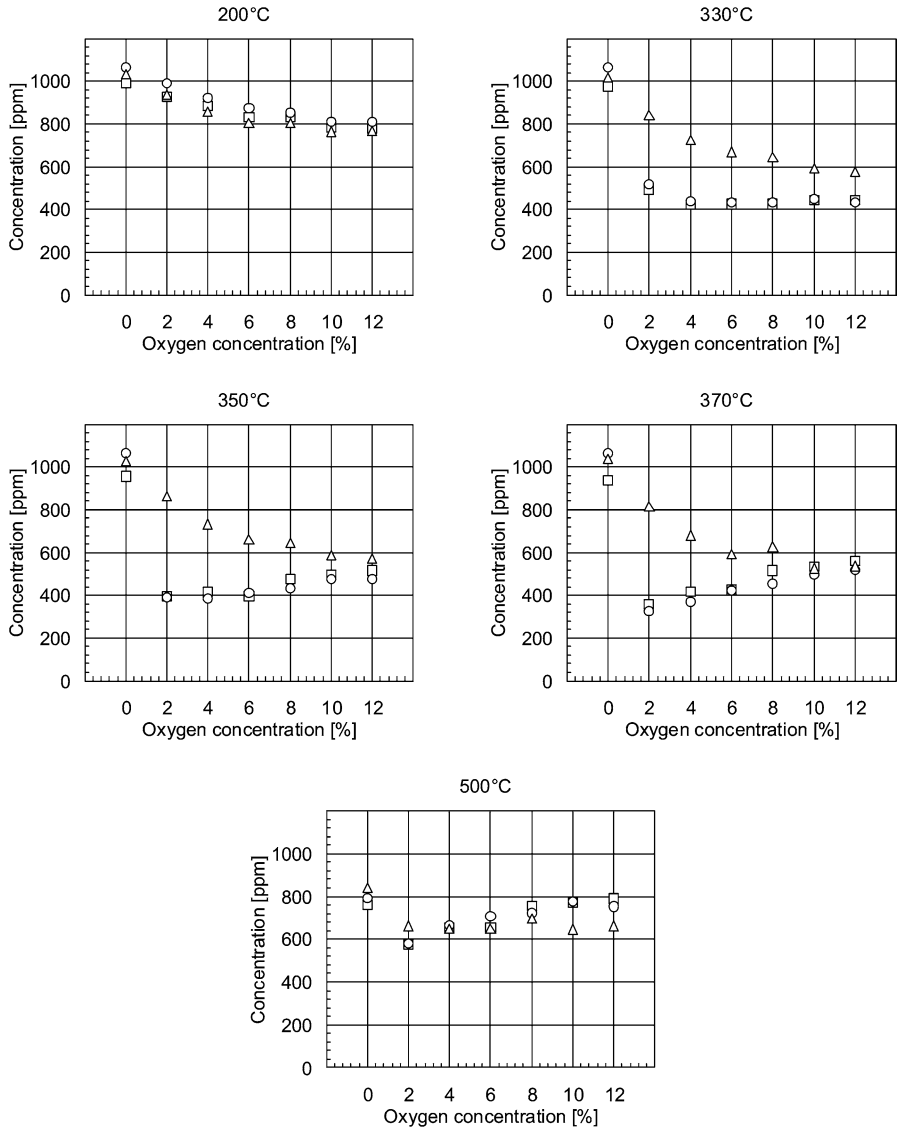

Fig. 2. NO_x concentration at the reactor outlet with propene at 200–500 °C. CuFER + AgMOR (○); CuFER + HZSM-5 (□); CoFER + AgMOR (△). Gas inlet composition: 1000 ppm NO, 1067 ppm C_3H_6 and 0–12% O_2. Balanced with N_2.

NO_x concentrations at the reactor outlet with propene and isooctane are shown in Figs. 2 and 3. When the NO_x reduction was compared for the same sample with isooctane and propene, propene was the more effective reducing agent in all cases. With propene as the reducing agent, very similar results were obtained for CuFER + AgMOR and CuFER + HZSM-5, but somewhat higher NO_x concentrations were observed for CoFER + AgMOR. This order of performance was changed somewhat for isooctane. At 200 and 500 °C, no significant differences were seen among the samples. At the intermediate temperatures, CuFER + HZSM-5 had the lowest NO_x concentrations, followed by CoFER + AgMOR and then CuFER + AgMOR. Based on these observations, the overall reaction rate of NO_x reduction with propene appears to be governed by a process in the ferrierite extrudate. The second zeolite in the mixture influenced the results only when isooctane was used.

Before the differences in sample performance can be attributed to variations in intracrystalline diffusivity or catalyst activity, the effects of deviations in test conditions and in physical properties of the samples (Tables 1 and 2) must be taken into account. Identical test conditions (i.e., gas composition, gas flow, equilibrium time, and inlet gas temperature) were used. Because the hydrocarbon concentrations were rather high, the exotherms over the reactor bed were significant (up to 30 °C). However, these large exotherms were connected with high conversions of hydrocarbon; that is, they were observed only at 500 °C for isooctane. In the isooctane experiments at lower temperatures, the exotherms were <4 °C. This means that large exotherms were observed only when there were negligible variations in NO_x conversion between CuFER + AgMOR and CuFER + HZSM-5, and thus the differences in conversion cannot be attributed to deviations in test conditions.

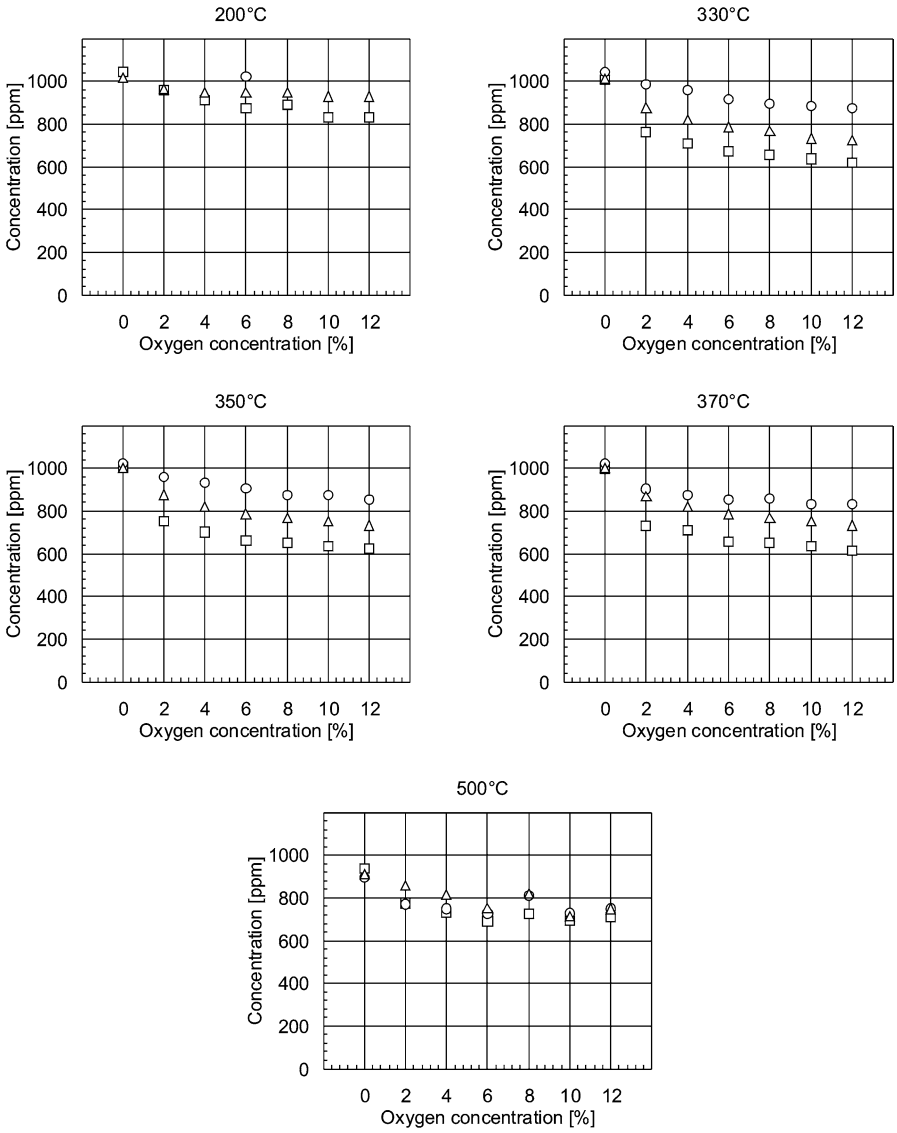

Fig. 3. NO_x concentration at the reactor outlet with isooctane at 200–500 °C. CuFER + AgMOR (○); CuFER + HZSM-5 (□); CoFER + AgMOR (△). Gas inlet composition: 1000 ppm NO, 400 ppm i-C_8H_{18} and 0–12% O_2. Balanced with N_2.

The bed volumes were the same for all samples, but due to differences in packing, the catalyst weights were not the same. Because of the deviations in catalyst amounts, the rate of external mass transfer varied for the samples. The weight of CuFER + HZSM-5 was 90.2% of the weight of CuFER + AgMOR. Estimating the external mass transfer coefficient with Colburn j_D factors [26], the coefficient was approximately 3.7% higher for CuFER + HZSM-5 than for CuFER + AgMOR. However, a lower amount of sample also corresponded to a lower external surface area. The external surface area of the extrudates in the CuFER + HZSM-5 sample was 92.7% of that in the CuFER + AgMOR sample. The higher external mass transfer coefficient in the CuFER + HZSM-5 sample was completely offset by the higher external surface area in CuFER + AgMOR. All other factors being equal, the observed conversion thus would be lower for the CuFER + HZSM-5. Hence the differences in NO_x conversion cannot be attributed to differences in catalyst weight.

Apart from the difference in sample weights evaluated earlier, there were also some physical variations between the four types of extrudates (see Table 1). The difference between AgMOR and HZSM-5 is of particular interest, because the variation in NO_x conversion with isooctane has been attributed to this difference. In comparison, AgMOR has larger pores and higher porosity in the external pore system (i.e., the pore system outside the zeolite framework), which corresponds to a higher effective diffusivity in the extrudate. Thus the observed conversion would be higher for the sample containing AgMOR if all other factors were equal. The AgMOR extrudates also have smaller zeolite crystallites than the HZSM-5 extrudates. With equal effective intracrystalline diffusivity, the intracrystalline pore diffusion limitation would be greater for the HZSM-5 extru-

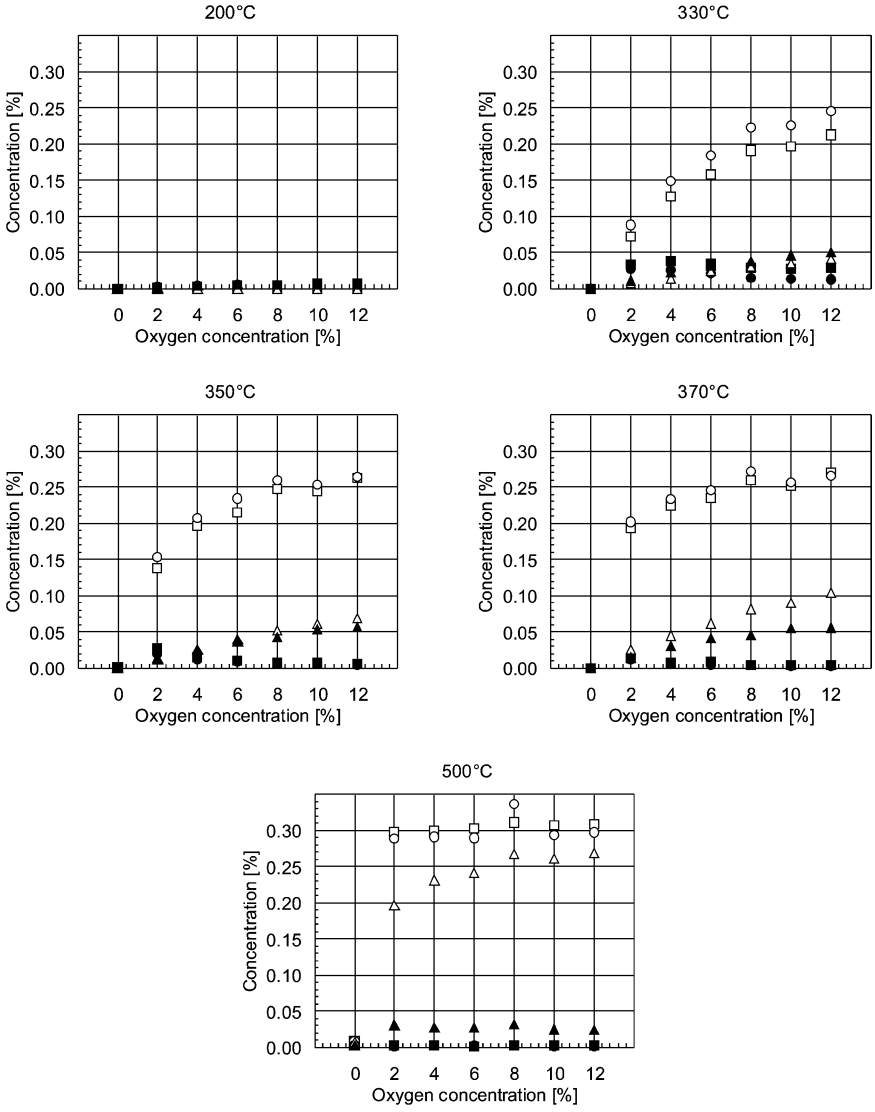

Fig. 4. CO and CO_2 concentrations at the reactor outlet with propene at 200–500 °C. CuFER + AgMOR with CO_2 (○) or CO (●); CuFER + HZSM-5 with CO_2 (□) or CO (■); CoFER + AgMOR with CO_2 (△) or CO (▲). Gas inlet composition: 1000 ppm NO, 1067 ppm C_3H_6 and 0–12% O_2. Balanced with N_2.

dates, because of longer diffusion paths, and the NO_x conversion would be higher for the mixture containing AgMOR if all other factors were equal.

From this discussion, it can be concluded that CuFER + HZSM-5 had the highest NO_x conversion with isooctane, despite the physical differences in Tables 1 and 2. Because the differences in NO_x conversion do not correlate with the differences in physical properties of the extrudates, these findings must be due to variations in catalyst activity or the intracrystalline diffusion coefficient.

3.2. Hydrocarbon oxidation

The gas composition in these experiments was chosen so there would be excess oxygen (when present) compared with hydrocarbon and NO_x and excess hydrocarbon compared with NO_x. This makes it possible to examine hydrocarbon oxidation separately from NO_x reduction.

Starting with the propene experiments, the concentrations of CO_2 and CO are shown in Fig. 4, and the corresponding hydrocarbon concentrations are shown in Fig. 6. CO_2 production rises with increasing temperature and increasing oxygen concentration. At 200 °C, no formation of CO_2 was observed for any sample. At 330 °C and above, CuFER + AgMOR and CuFER + HZSM-5 had high CO_2 concentrations. The CoFER + AgMOR yielded modest CO_2 concentrations at 350 and 370 °C and high concentrations at 500 °C. The total hydrocarbon concentrations showed an opposite trend to that of CO_2 production, with increasing temperature and oxygen concentration resulting in decreased hydrocarbon concentration. Note that even at the highest temperature, with maximum oxygen concentration and with propene, some hydrocarbon was still reaching the reactor outlet. This indicates an external mass transfer limitation.

Based on the total hydrocarbon and CO_2 concentrations, the propene conversion was identical for CuFER +

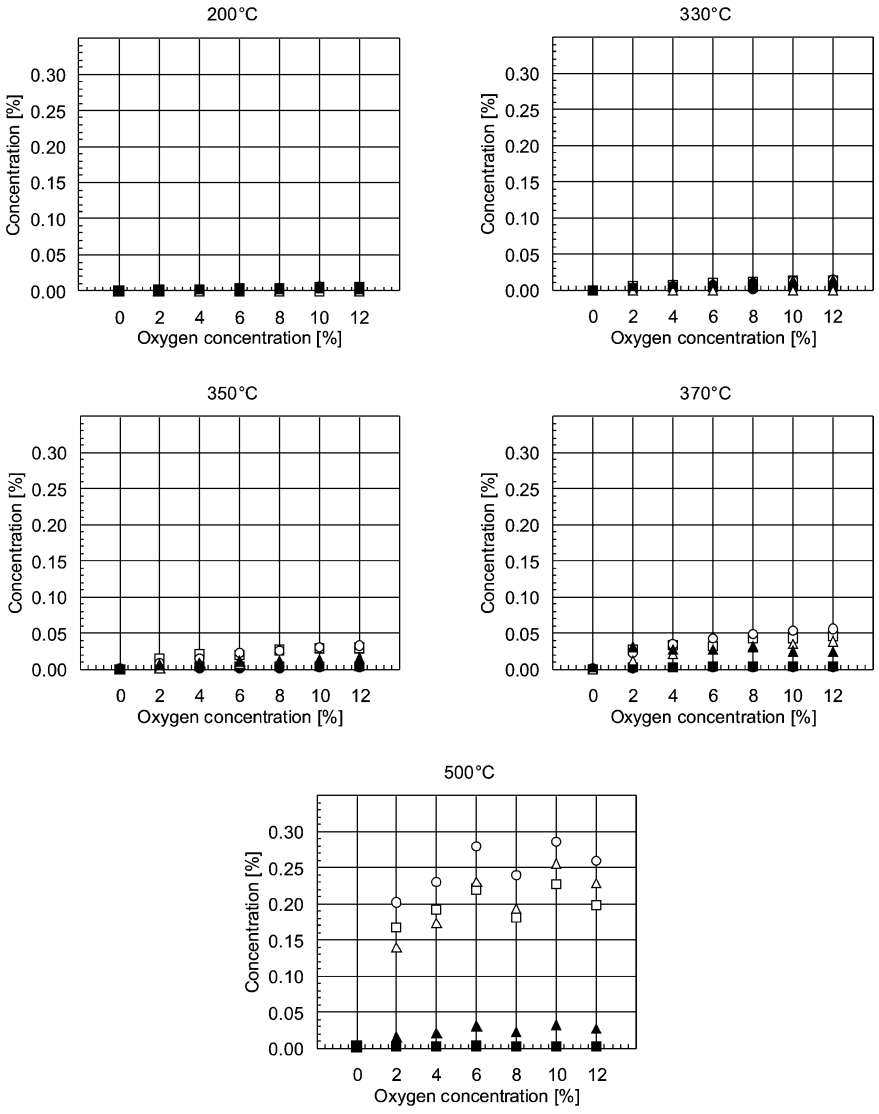

Fig. 5. CO and CO_2 concentrations at the reactor outlet with isooctane at 200–500 °C. CuFER + AgMOR with CO_2 (○) or CO (●); CuFER + HZSM-5 with CO_2 (□) or CO (■); CoFER + AgMOR with CO_2 (△) or CO (▲). Gas inlet composition: 1000 ppm NO, 400 ppm i-C_8H_{18} and 0–12% O_2. Balanced with N_2.

AgMOR and CuFER + HZSM-5, and lower for CoFER + AgMOR. This indicates that these variations was due to differences between the CuFER and CoFER extrudates. Apart from different ions, the ion concentration in the CoFER extrudate was only 7.9% of the concentration in CuFER. Based on the observed CO_2 concentrations and assuming a plug flow reactor and a first-order reaction, the apparent rate constant for propene oxidation over these two samples can be estimated. For propene conversions up to 70%, the apparent rate constant for the sample containing CoFER was between 6.3 and 11.3% of the constants observed for the sample containing CuFER. This indicates that the major difference in propene oxidation was due to the differing number of oxidation sites in these samples. Although CoFER appears to be as good a propene oxidation catalyst as CuFER, it was harder to introduce sufficient numbers of counter ions.

The production of CO was generally significantly lower than that of CO_2. As shown in Fig. 4, CO production was observed over the CoFER + AgMOR sample at 350 °C and above, whereas all three samples had some CO production at 330 °C. Adsorbed CO is assumed to be formed as an intermediate in the complete oxidation of the hydrocarbon. If the rate of CO oxidation is too slow, then the adsorbed CO can desorb and cause CO emissions, as was observed. The observed CO concentrations over the CoFER + AgMOR sample at 350 °C and above thus appears to indicate that the number of metal sites in the CoFER extrudate was too low to achieve complete oxidation of the hydrocarbons at these temperatures. The CO observed for all samples at 330 °C indicate that not even the CuFER extrudate was sufficiently active for the CO oxidation.

The results from the isooctane experiments are shown in Figs. 5 (for CO and CO_2 concentration) and 7 (for total hy-

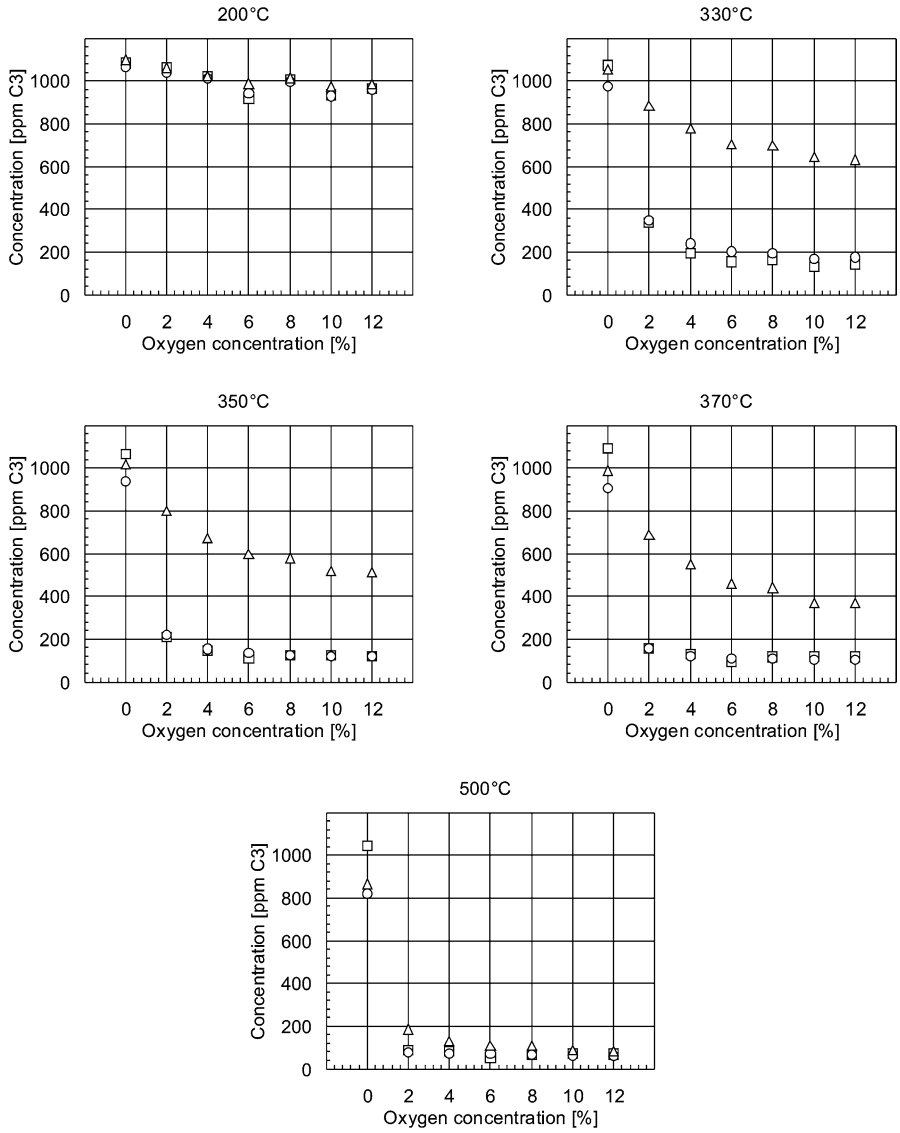

Fig. 6. Hydrocarbon concentration at the reactor outlet with propene at 200–500 °C. CuFER + AgMOR (○); CuFER + HZSM-5 (□); CoFER + AgMOR (△). Gas inlet composition: 1000 ppm NO, 1067 ppm C_3H_6 and 0–12% O_2. Balanced with N_2.

drocarbon concentration). Because the FID detector was calibrated for C_3 equivalence, the 400-ppm feed concentration of isooctane corresponds to a total hydrocarbon concentration of 1067 ppm C_3 in Fig. 7. Comparing these results with those for propene shows that CO_2 formation was significantly lower at all temperatures, indicating a lower rate of oxidation for isooctane.

The results from the isooctane experiments given in Fig. 5 show low concentrations of CO at all temperatures and low concentrations of CO_2 below 500 °C. But despite this finding, the total hydrocarbon concentration in Fig. 7 decreased with rising oxygen concentration at temperatures between 330 and 370 °C. This oxygen dependence indicates that an oxidation was occurring. Because the carbon balance does not add up, at least a portion of the oxidation product must be trapped in the sample. This trapped oxidation product cannot be CO_2, because CO_2 was readily emitted from the samples in the propene oxidation experiments. Thus the trapped reaction product is assumed to be a partially oxidized hydrocarbon species. A possible explanation for this behavior is that when the isooctane was partially oxidized, it broke down into smaller species that were adsorbed in the ferrierite pore system.

3.3. NO_x reduction

Returning to the NO_x concentration results during the propene experiments in Fig. 2, a minimum was found for the CuFER + AgMOR and CuFER + HZSM-5 samples at 2% oxygen at 350 °C and above. At 330 °C, the same samples had a wide minimum around 6% oxygen, whereas at 200 °C, the NO_x concentration decreased continuously with increasing oxygen concentration, within the range studied. For the CoFER + AgMOR mixture, the oxygen concentra-

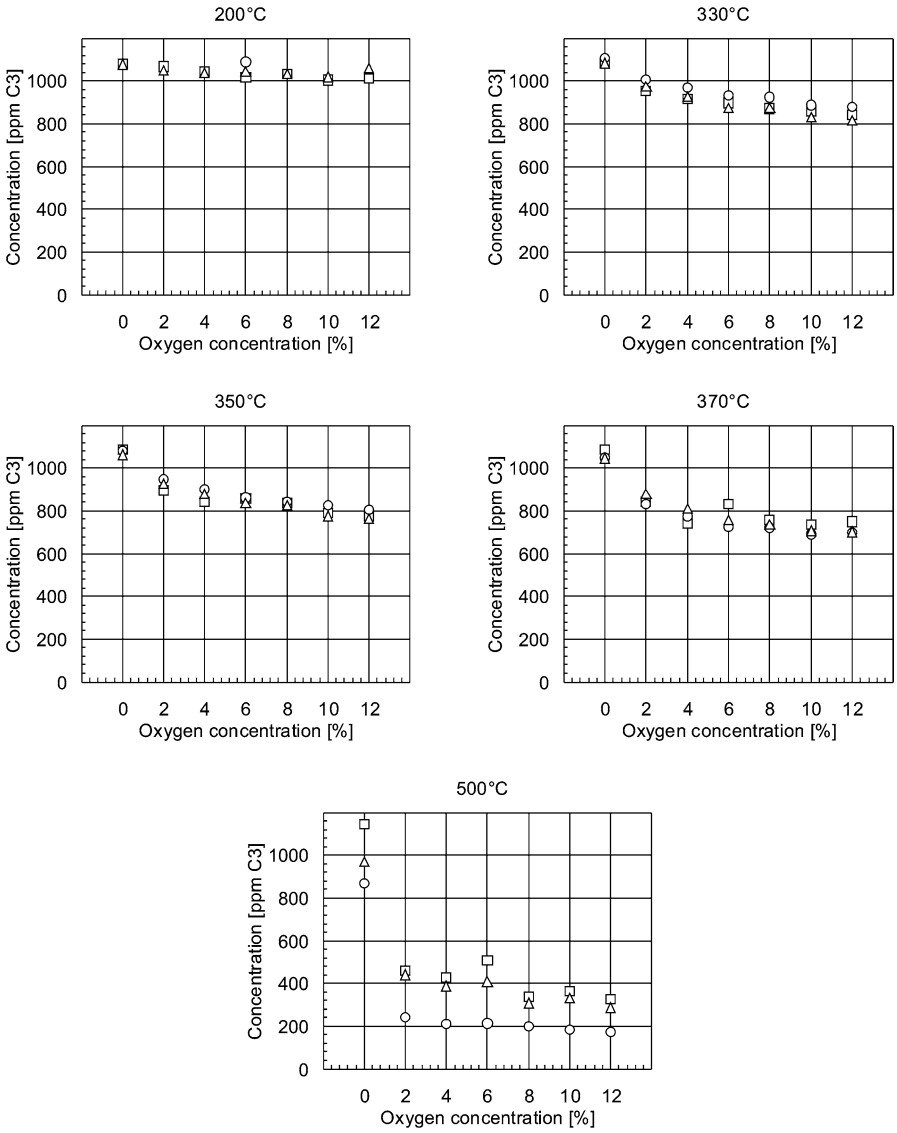

Fig. 7. Hydrocarbon concentration at the reactor outlet with isooctane at 200–500 °C. CuFER + AgMOR (○); CuFER + HZSM-5 (□); CoFER + AgMOR (△). Gas inlet composition: 1000 ppm NO, 400 ppm i-C_8H_{18} and 0–12% O_2. Balanced with N_2.

tion had a minor effect at 500 °C when oxygen was present. At lower temperatures, increasing the oxygen concentration decreased the NO_x concentration. The corresponding concentrations of NO and NO_2 are shown in Fig. 8. Almost all of the NO_x observed was in the form of NO. Elevated concentrations of NO_2 were found for all samples at 200 °C and for CuFER + AgMOR and CuFER + HZSM-5 at 500 °C.

The oxygen-dependent minimum in the NO_x concentration observed for CuFER + AgMOR and CuFER + HZSM-5 with propene can be attributed to the rates of reactions (1) and (3) in Fig. 1. Low oxygen concentrations result in a lower rate of NO_2 formation (reaction (1)), whereas high oxygen concentrations result in high hydrocarbon consumption (reaction (3)). The effect of limited oxygen concentration on reaction (1) was most pronounced at 200 °C, at which maximum NO_x reduction was observed at the highest oxygen concentration. At higher temperatures, the rate of hydrocarbon oxidation increases, and the hydrocarbon concentration limits the NO_x reduction. The lower NO_x reduction for CoFER + AgMOR compared with the other samples is attributed to a lower selectivity for nitrogen formation (reactions (2a) and (2b)). The alternative explanation, that the NO_2 formation (reaction (1)) was lower for CoFER + AgMOR, is not likely, because it was found to have a high NO_2 formation already at 200 °C (Fig. 9). The reason why no minimum in NO_x concentration was found for this sample is that the hydrocarbon oxidation (reaction (3)) was slower due to the lower number of active sites, as discussed earlier.

The limited oxidation of isooctane observed means that there was no limitation in hydrocarbon supply for the nitrogen formation reaction (reaction (2a)). Hence, when the oxygen concentration was varied, no minimum in the NO_x concentration could be observed in Fig. 3. The NO_x concentrations were higher with isooctane than with propene,

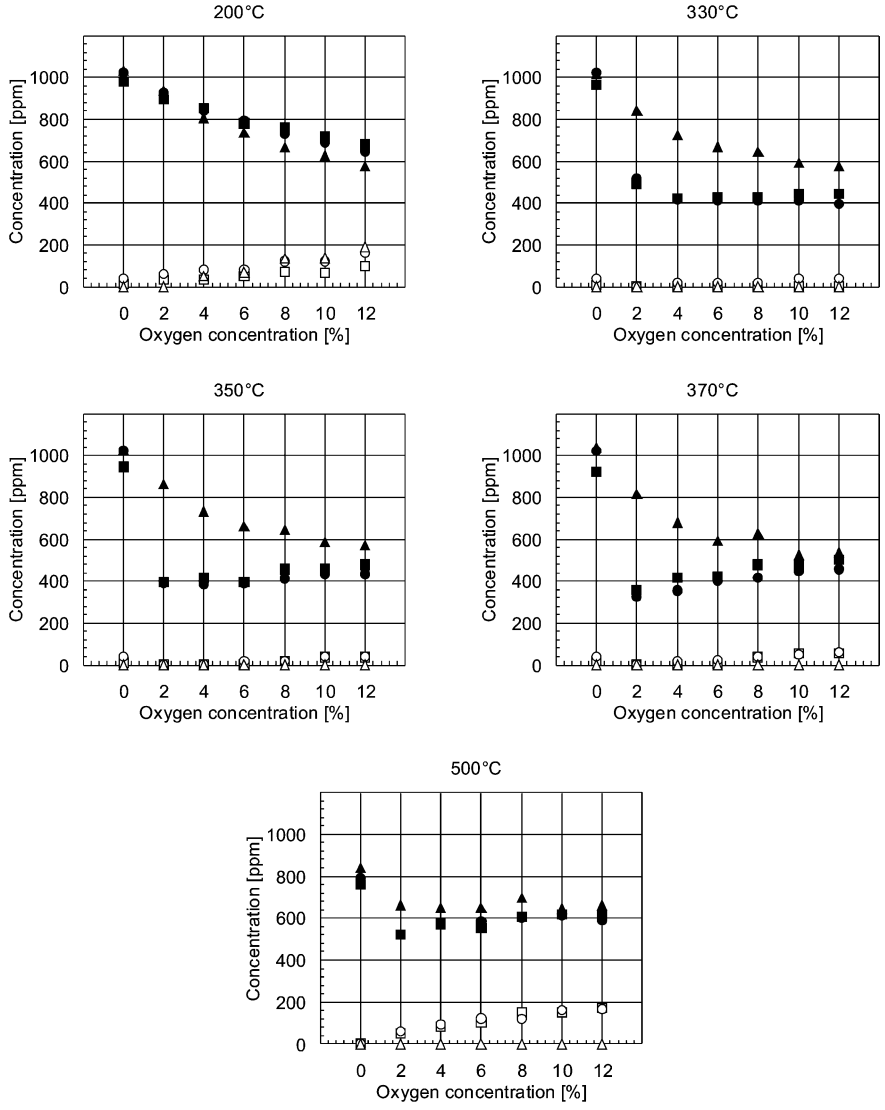

Fig. 8. NO and NO_2 concentrations at the reactor outlet with propene at 200–500 °C. CuFER + AgMOR with NO_2 (○) or NO (●); CuFER + HZSM-5 with NO_2 (□) or NO (■); CoFER + AgMOR with NO_2 (△) or NO (▲). Gas inlet composition: 1000 ppm NO, 1067 ppm C_3H_6 and 0–12% O_2. Balanced with N_2.

however. This means that reaction (2a) must be slower with isooctane than with propene. Still, almost no NO_2 was observed at temperatures >200 °C (Fig. 9), because the NO formation reaction (reaction (2b)) was consuming the NO_2. Thus the variations in NO_x reduction performance between the samples can be attributed to the selectivity for NO_2 to form nitrogen instead of NO when isooctane was used. When combined with CuFER, the structure of HZSM-5 appears to be better suited for reaction (2a) than AgMOR. An alternative explanation, that the entire reaction scheme was governed by the reaction rates in a single component (i.e., the CuFER component did not affect the overall performance), is not likely based on the single-component studies reported previously [21,23]. Thus with isooctane, the mixtures behaved as dual pore system catalysts.

An important difference between these structures is that whereas the framework of HZSM-5 (the MFI structure) has a three-dimensional pore system, the framework of AgMOR is one-dimensional. Strongly adsorbing species inside the AgMOR crystallites could thus block the diffusion paths for other species. Other possible explanations for the better performance of the sample containing HZSM-5 include a higher affinity for one or more of the reactants, higher diffusivities, and a higher number of active sites.

At 330 °C with isooctane, the NO_x concentration was lower in CoFER + AgMOR than in CuFER + AgMOR. This is assumed to be due to the higher NO_2 formation for CoFER + AgMOR than for CuFER + AgMOR (reaction (1)) and thus the higher rate of reaction (2a). The same effect was not found with propene, for which CuFER + AgMOR was more active for NO_x reduction than CoFER + AgMOR. The reason for this difference is that the NO_x reduction reactions ((2a) and (2b)) occurred in the ferrierite extrudate in the presence of propene and in AgMOR (or HZSM-5) in the presence of isooctane.

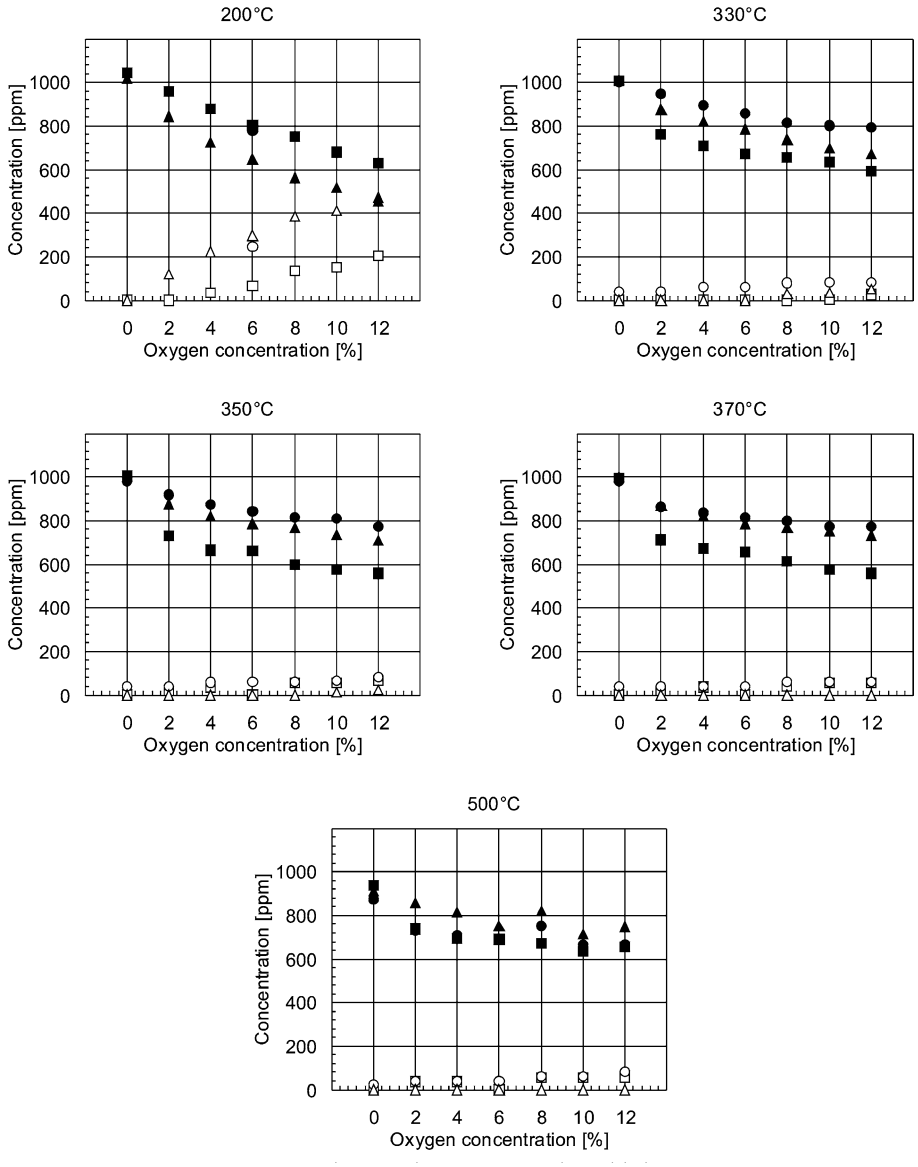

Fig. 9. NO and NO_2 concentrations at the reactor outlet with isooctane at 200–500 °C. CuFER + AgMOR with NO_2 (○) or NO (●); CuFER + HZSM-5 with NO_2 (□) or NO (■); CoFER + AgMOR with NO_2 (△) or NO (▲). Gas inlet composition: 1000 ppm NO, 400 ppm i-C_8H_{18} and 0–12% O_2. Balanced with N_2.

For both reducing agents, the NO_x concentrations were lower at 370 °C than at 500 °C (Figs. 2 and 3). At the higher temperature, the formation of NO_2 (reaction (1)) is limited by the thermodynamic equilibrium. This explains the increase in NO_x concentration observed for all samples with isooctane and for CoFER + AgMOR with propene. However, the thermodynamic limitation cannot explain the increase in NO_x concentration seen for CuFER + AgMOR and CuFER + HZSM-5 with propene, because significant concentrations of NO_2 were observed at 500 °C (Fig. 8). The NO_x reduction for these samples at 500 °C in the presence of propene was thus limited by the hydrocarbon concentration rather than by the NO_2 was not. Supporting this theory is the earlier observation that propene oxidation was limited by external mass transfer.

The foregoing model cannot explain the decrease in NO_x concentration in the absence of oxygen at 500 °C for propene and isooctane. Instead, this is attributed to a direct reaction between NO and the hydrocarbon. Because no NO_x reduction was observed in the absence of oxygen below 500 °C, the activation energy must be so high as to make the rate of this reaction negligible for this temperature range.

In the envisaged application for dual pore system catalysts, SO_2 and water will be present. Water has been shown to cause a reversible inhibition on related metal-containing zeolite systems (CuZSM-5 [24], CoFER [27], and Ce/AgZSM-5 [28]), and a similar inhibition may be expected on the systems studied here. It is well known that more severe hydrothermal conditions cause dealumination of zeolites that becomes more severe with decreasing

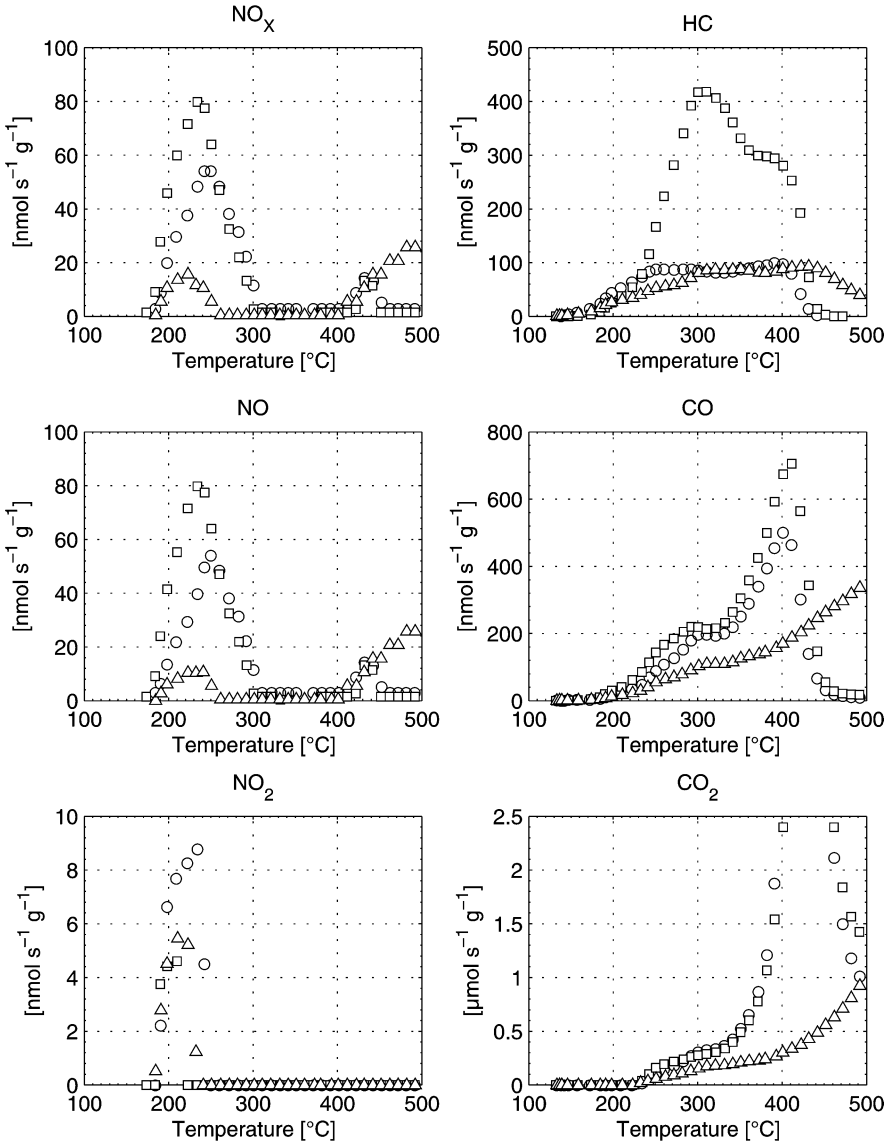

Fig. 10. Molar release rates from samples during temperature programmed reaction ramps after saturation in 1000 ppm NO, 1067 ppm C_3H_6 and 6% O_2 at 120 °C. Samples were degassed for 10 min at 120 °C and heated to 500 °C in 6% O_2 at 10 °C/min. CuFER + AgMOR after 12.5 h on stream (○); CuFER + HZSM-5 after 8.5 h on stream (□); CoFER + AgMOR after 12.5 h on stream (△).

SiO_2/Al_2O_3 ratio of the zeolite. We thus would expect the ZSM-5 and MOR components to have similar hydrothermal stabilities and the FER components to have lower stability. A recent study found that a CuFER sample was hydrothermally stable for at least 20 h at 600 °C [29]. Thus, hydrothermal deactivation would not be expected within the temperature range studied.

The sensitivity of Co-exchanged zeolites toward SO_2 in the absence of water has been found to depend on the zeolite structure, whereas the lean NO reduction with methane was more affected over CoFER than over CoZSM-5. When combining SO_2 and water, both samples were significantly deactivated [27]. Martens et al. showed that the deNO_x performance of Ag/H-MOR and Ag/H-FER zeolites remained unaffected by the presence of 150 ppm SO_2 [30]. SO_2 has been shown to reversibly poison CuZSM-5 catalysts [24], and a similar effect may be expected for the CuFER. To our knowledge, the effect of SO_2 on the HC reduction of NO_x over HZSM-5 has not been studied; however, in combination with Pt/ZrO_2, the NO reduction with hydrogen was only slightly affected by SO_2 [31]. Based on these observations, we would expect the presence of water and SO_2 to inhibit the dual pore system catalysts studied here but not alter their relative order of performance.

3.4. Temperature-programmed studies

Fig. 10 shows temperature-programmed reaction ramps of the zeolite mixtures after saturation in reactant gas mixture at 120 °C. Starting with the hydrocarbon graph, there clearly was only a small difference between the CuFER and CoFER samples containing AgMOR, whereas the HZSM-5-

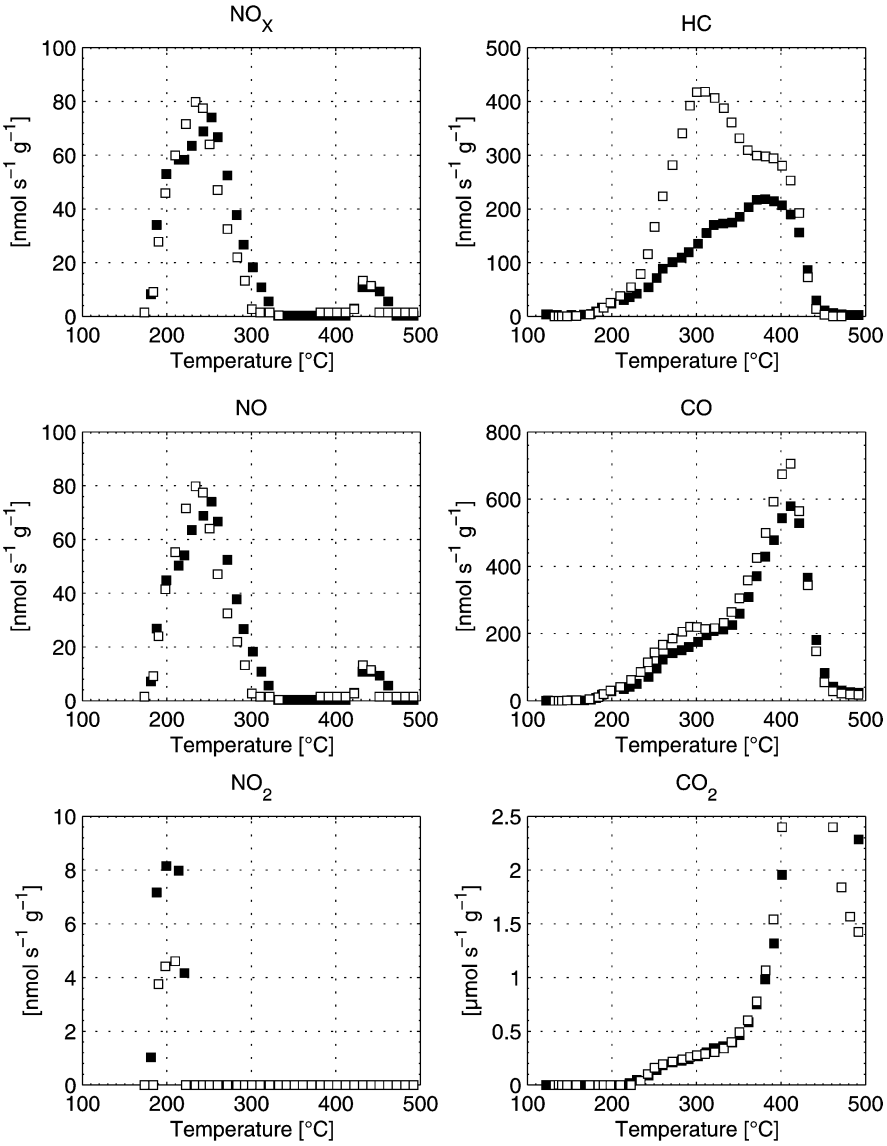

Fig. 11. Molar release rates from samples during temperature programmed reaction ramps after saturation in 1000 ppm NO, 1067 ppm C_3H_6 and 6% O_2 at 120 °C. Samples were degassed for 10 min at 120 °C and heated to 500 °C in 6% O_2 at 10 °C/min. CuFER + HZSM-5 after 8.5 h on stream (□) and after 28 h on stream (■).

containing sample had a significantly higher release. Noteworthy is that the CoFER + AgMOR sample released some hydrocarbons above 450 °C, in contrast to the other two samples. For CO and CO_2, there was only a small difference between the two samples containing CuFER, whereas the CoFER-containing sample released significantly lower amounts of these oxidation products, presumably due to the lower number of oxidation sites in CoFER as discussed earlier.

NO_x was released in two temperature regions, one around 200–300 °C because the hydrocarbon was not activated at that temperature, and the other around 420–500 °C due to the NO/NO_2 equilibrium favoring the formation of the less-reactive NO. At high temperature, the CoFER + AgMOR sample released more NO than the two CuFER-containing samples, suggesting that NO_x was more strongly bound to CoFER than to CuFER. This suggestion is supported by the lower release of NO_x observed from the CoFER sample at low temperatures. In addition, the CoFER + AgMOR sample released NO_x with a significantly higher NO_2/NO ratio than CuFER + AgMOR, which in turn had a higher ratio than CuFER + HZSM-5. This supports our previous observation that CoFER has a higher NO_2 formation rate than CuFER. The difference between the two CuFER-containing samples was attributed to a higher rate of NO_2 reduction over the HZSM-5 containing sample. The higher rate is due to a lower required temperature for hydrocarbon activation over the HZSM-5-containing sample, as is evident from the CO and CO_2 graphs. The TPR results thus support the earlier discussion regarding the reaction mechanism.

Fig. 11 shows the TPR results for the CuFER + HZSM-5 sample after different times on stream. The most conspicu-

ous difference is seen in the hydrocarbon graph. Even though the CO and CO_2 curves appeared less affected, hydrocarbon release was significantly lower after 28 h on stream; in particular, the low-temperature peak almost disappeared. The NO_2 release peak was almost doubled, due to either a decrease in NO_2 reduction rate or an increase in NO oxidation rate. But this had only a minor effect on the NO_x and NO release curves, where the peaks at low temperature were only slightly broadened. In the tested time and temperature region, the NO_x reduction performance of this sample thus appears stable.

Finally, the NO_x reduction studies were performed using a 1:1 weight ratio of the individual components. Because there was no breakthrough of NO_2 in the most active systems, increasing the NO oxidation component in the mixture would likely further increase nitrogen formation.

4. Conclusions

Physical mixtures of zeolite extrudates were found to exhibit lean NO_x reduction capability with propene and isooctane. For propene, the overall rate of NO_x reduction was determined by a process in the extrudate containing ferrierite, whereas NO_x reduction with isooctane was influenced by both the extrudates. These mixtures were thus found to act as dual pore system catalysts when isooctane was used as the reducing agent.

For both reducing agents, NO_2 acted as an intermediate for the NO_x reduction. With propene, the CuFER-containing mixtures were more active in the reduction than the CoFER-containing mixture, due to higher selectivity for NO_2 to form nitrogen rather than NO. The samples containing CuFER showed a maximum in NO_x conversion at an intermediate oxygen concentration, due to competition between NO_2 formation and consumption of the reducing agent.

When isooctane was used, the CuFER + HZSM-5 mixture had the highest NO_x conversion, despite this sample's more severe external and internal mass transfer limitations. Generally, all samples had a lower selectivity for NO_2 reacting to nitrogen with isooctane than with propene. The differences in NO_x reduction between the samples for isooctane are again attributed to differing selectivity for complete reduction. The reason for this higher selectivity awaits further investigation.

Acknowledgments

The authors are pleased to acknowledge financial support from the Swedish Research Council for Engineering Sciences and from the KK Foundation through the MARCHAL Program. They also thank Eka Chemicals and Tosoh for providing the zeolite samples. The work reported in this paper was conducted at the Competence Centre for Catalysis, which is supported by the Swedish Energy Agency and member companies AB Volvo, Saab Automobile AB, Johnson Matthey CSD, Perstorp AB, AVL-MTC AB, Albemarle Catalysts, and the Swedish Space Administration.

References

[1] United Nations, United Nations Framework Convention on Climate Change, May 1992.
[2] United Nations, http://unfccc.int/resource/conv/ratlist.pdf, 9 May 2005.
[3] United Nations, Kyoto Protocol to the United Nations Framework Convention on Climate Change, December 1997.
[4] Association des constructeurs européens d'automobiles, ACEA's CO_2 Commitment, December 2002.
[5] A. König, G. Herding, B. Hupfeld, Th. Richter, K. Weidmann, Top. Catal. 16/17 (2001) 23.
[6] E. Jobson, Top. Catal. 28 (2004) 191.
[7] M.D. Amiridis, T. Zhang, R.J. Farrauto, Appl. Catal. B 10 (1996) 203.
[8] V.I. Parvulescu, P. Grange, B. Delmon, Catal. Today 46 (1998) 233.
[9] Y. Traa, B. Burger, J. Weitkamp, Micropor. Mesopor. Mater. 30 (1999) 3.
[10] M. Iwamoto, N. Mizuno, H. Yahiro, Stud. Surf. Sci. Catal. 75 (1992) 1285.
[11] X. Wang, H.Y. Chen, W.M.H. Sachtler, J. Catal. 197 (2001) 281.
[12] T. Tabata, H. Ohtsuka, L.M. F Sabatino, G. Bellussi, Micropor. Mesopor. Mater. 21 (1998) 517.
[13] X. Feng, H.K. Hall, J. Catal. 166 (1997) 368.
[14] F. Heinrich, C. Schmidt, E. Löffler, W. Grunert, Catal. Commun. 2 (2001) 317.
[15] H. Hamada, Y. Kintaichi, M. Sasaki, T. Ito, Appl. Catal. 64 (1990) L1.
[16] I. Halasz, A. Brenner, K.Y.S. Ng, Y. Hou, J. Catal. 161 (1996) 359.
[17] H. Hamada, Y. Kintaichi, M. Sasaki, T. Ito, M. Tabata, Appl. Catal. 70 (1991) L15.
[18] H.H. Ingelsten, D. Zhao, A. Palmqvist, M. Skoglundh, J. Catal. 232 (2005) 68.
[19] J.O. Petunchi, G. Sill, W.K. Hall, Appl. Catal. B 2 (1993) 303.
[20] M. Misono, Y. Hirao, C. Yokoyama, Catal. Today 38 (1997) 157.
[21] J.A. Martens, A. Cauvel, F. Jayat, S. Vergne, E. Jobson, Appl. Catal. B 29 (2001) 299.
[22] E. Jobson, J.A. Martens, A. Cauvel, F. Jayat, European Patent 1044056, to Volvo Car Corporation.
[23] T. Holma, A. Palmqvist, M. Skoglundh, E. Jobson, Appl. Catal. B 48 (2004) 95.
[24] A.P. Walker, Catal. Today 26 (1995) 107.
[25] R. Brosius, J.A. Martens, Top. Catal. 28 (2004) 119.
[26] R.B. Bird, W.E. Stewart, E.N. Lightfoot, Transport Phenomena, Wiley, New York, 1960, p. 647.
[27] Y. Li, J.N. Armor, Appl. Catal. B 5 (1995) L257.
[28] Z. Li, M. Flytzani-Stephanopoulos, Appl. Catal. B 22 (1999) 35.
[29] K. Rahkamaa-Tolonen, T. Maunula, M. Lomma, M. Huuhtanen, R.L. Keiski, Catal. Today 100 (2005) 217.
[30] J.A. Martens, A. Cauvel, A. Francis, C. Hermans, F. Jayat, M. Remy, M. Keung, J. Lievens, P.A. Jacobs, Angew. Chem. 37 (1998) 1901.
[31] T. Nanba, K. Sugawara, S. Masukawa, J. Uchisawa, A. Obuchi, Ind. Eng. Chem. Res. 44 (2005) 3426.